Annual Progress Report for JFY 2008

March 23, 2009

# CDF Experiment

Spokespersons
Japan F. Ukegawa (University of Tsukuba)
U.S.A. R. Roser (Fermilab) and J. Konigsberg (University of Florida)

The CDF experiment at the Fermilab Tevatron proton-antiproton collider continued to accumulate high-statistics data and produce rich physics results in 2008. The accelerator performance was the best ever achieved, surpassing the previous records in virtually every category. The instantaneous luminosity at the beginning of the stores now consistently exceeds $\mathcal{L} = 3 \times 10^{32}$ cm$^{-2}$ s$^{-1}$, with a record luminosity of $3.6 \times 10^{32}$ cm$^{-2}$ s$^{-1}$ in December 2008 (Figure 1 (top)). A weekly integrated luminosity in excess of 60 pb$^{-1}$ has also been achieved regularly. The total integrated luminosity in the calendar year 2008 amounted to about 2.2 fb$^{-1}$ and the Run II total to date has exceeded 6.2 fb$^{-1}$ (Figure 1 (bottom)).

The upgraded CDF detector has been operational very successfully with high efficiency. The integrated luminosity recorded by CDF amounts to 5.1 fb$^{-1}$, roughly 45 times that of Run I (Figure 2). We expect to collect a total of about 7 fb$^{-1}$ at the end of US fiscal year 2009, and 9 fb$^{-1}$ at the end of 2010 if the Tevatron running continues. The CDF detector has been operating reliably, and it resulted in high efficiency in data taking.

CDF has analyzed up to 3.6 fb$^{-1}$ of data thus far, depending on data sets and physics topics, and many important and interesting results have emerged. In this report we summarize these physics results, with an emphasis on contributions from the Japan group.

## 1 Physics Results

### 1.1 Electroweak physics

The measurement of the $W^\pm$ boson mass using the Run-II data, $m_W = 80413 \pm 48$ MeV/$c^2$ [1], represents the single most precise measurement of the quantity, as illustrated in Figure 3. The impact of this measurement on constraints on the Higgs boson mass will be discussed later in this document. A measurement using 2.3 fb$^{-1}$ of data is under way, which is expected to achieve a statistical precision of 11 MeV/$c^2$ and a total precision of 25 MeV/$c^2$. Combined with top quark mass measurements, it will provide constraints on the Higgs boson mass with a relative precision of 20%.

Another area of study concerns pair production of gauge bosons. The unified electroweak theory has a non-Abelian gauge structure, resulting in self-couplings of the gauge bosons, such as the $W^+W^-Z^0$ and $W^+W^-\gamma$ vertices. Using high-statistics data available, rare gauge-boson pair production processes have been observed and studied. Associated production of a $W^{\pm}$ boson and a $Z^0$ boson was observed in 2006 for the first time. In 2008, pair production of $Z^0$ bosons was observed for the first time in hadron collisions. The study used 2 fb$^{-1}$ of data. The leptonic decays of one of the $Z^0$ bosons are used, while the second $Z^0$ boson is identified with either a charged lepton pair or a neutrino pair. The production cross section is measured to be $\sigma(\bar{p}p \to Z^0Z^0X) = 1.4\,^{+0.7}_{-0.6}$ pb, in agreement with a theory prediction of $1.4 \pm 0.1$ pb.

## 1.2 Top quark physics

The top quark and its properties have been studied extensively since its discovery by CDF in 1995. With increased statistics of Run-II data, these studies are now performed with high precision.

The top quark analyses with Run-II data include measurements of the mass and production cross section using various decay channels. The production cross section has been measured in di-lepton, lepton + jet and all-hadronic channels. The combined value is $\sigma(\bar{p}p \to t\bar{t}X) = 7.0 \pm 0.3 \pm 0.4 \pm 0.4$ pb [2]. It is in agreement with a next-to-leading order QCD calculation of $6.7\,^{+0.71}_{-0.88}$ pb for $m_t = 175$ GeV/$c^2$. N. Kimura and Y. Takeuchi (Tsukuba) have contributed to di-lepton channel analyses.

The top quark mass is extracted using various techniques and channels as well. By combining all measurements, CDF finds the top quark mass to be $m_t = 172.6 \pm 0.9 \pm 1.2$ GeV/$c^2$. The precision has long surpassed the Run-II (2 fb$^{-1}$) goal of 3 GeV/$c^2$ and is now better than 1%. Using also the measurements by the D0 experiment, we derive the combined top quark mass of $m_t = 173.1 \pm 0.6 \pm 1.1$ GeV/$c^2$ (March 2009).

As noted earlier, a measurement of the $W$ boson mass has been performed by CDF recently. Combining it with top quark mass measurements provides indirect information on the Higgs boson mass through electroweak radiative corrections. Figure 4 shows the results as of winter 2008. A constraint on the standard model Higgs boson mass is obtained to be $90\,^{+36}_{-27}$ GeV/$c^2$ at 68% CL, and is less than 163 GeV/$c^2$ at 95% CL (Figure 5).

Other production and decay properties of the top quark are also being studied, including $t\bar{t}$ spin correlations at production and the $W^{\pm}$ boson helicity in the decay. Y. Takeuchi (Tsukuba) has been working on spin correlations using the di-lepton channel. N. Kimura (Tsukuba) has studied $t\bar{t}$ production mechanism using the spin correlation. For $t\bar{t}$ production at the Tevatron it is expected that the parton subprocess $q\bar{q} \to t\bar{t}$ is dominant over the subprocess $gg \to t\bar{t}$, with a predicted fraction of 0.85 vs. 0.15. The two processes can be disentangled by using the spin correlation information, because they are in different spin states near threshold and the fact results in different azimuthal angle correlations between the $t$ and $\bar{t}$ decay products, notably the two charged leptons in the di-lepton channel. Figure 6 shows the observed angular distribution, along with fit results. The relative fraction of the gluon-gluon subprocess is measured to be $f_{gg} = 0.53\,^{+0.35}_{-0.37}\,^{+0.07}_{-0.08}$ [4], consistent with the prediction.

In hadron-hadron collisions top quarks are predominantly produced in pairs via the strong interaction. In addition, single top quarks can be produced by the electroweak interaction, for example via the subprocess $u\bar{d} \to W^{*+} \to t\bar{b}$. The process is interesting because the production cross section is proportional to the partial width $\Gamma(t \to W^+ b)$, and thus allows a direct determination of the CKM matrix element $|V_{tb}|$, with an expected precision of 15%. Evidence for single top-quark production was first presented in 2007. K. Nakamura (Tsukuba) has looked for single top production with an analysis optimized for the $s$-channel subprocess $q\bar{q}' \to W^{*+} \to t\bar{b}$ [5]. Figure 7 (left) shows the likelihood distribution of candidate events in the $s$-channel search. The analysis extracts the production cross section of $\sigma = 1.5\,^{+0.9}_{-0.7}$ pb, with a probability of background fluctuation of 0.022, or a 2.0 standard deviation effect. Other analysis channels and techniques are combined, and the cross section is measured to be $\sigma = 2.3\,^{+0.6}_{-0.5}$ pb [6] and is illustrated in Figure 7 (right), which includes both $s$-channel and $t$-channel contributions. Also, the CKM matrix element is determined to be $|V_{tb}| = 0.91 \pm 0.11 \pm 0.07$, or $|V_{tb}| > 0.71$ at 95% CL.

## 1.3 Bottom quark physics

In 2006 CDF observed the particle-antiparticle oscillations of the $B_s^0$ meson and measured their frequency $\Delta m_s$ [7]. It has led to a very precise determination of the elements of the CKM matrix, $|V_{td}/V_{ts}| = 0.2060 \pm 0.0007\,^{+0.0081}_{-0.0060}$, and provided a stringent test of the Kobayashi-Maskawa picture of CP violation.

The observation now allows us to look for CP violation in $B_s^0$-$\bar{B}_s^0$ mixing, which modulates with the frequency $\Delta m_s$. The decay mode $B_s^0 \to J/\psi\,\phi$ is the most useful for this purpose. Figure 8 (left) shows the signal, and Figure 8 (right) illustrates the allowed region in the $\beta_s$-$\Delta\Gamma$ plane, along with the standard model prediction, where $\beta_s$ is the CP-violating phase in $B_s^0$-$\bar{B}_s^0$ mixing and $\Delta\Gamma$ is the width difference in the mass/lifetime eigenstates of the $B_s^0$-$\bar{B}_s^0$ system. This is the first constraint obtained for the phase $\beta_s$ [8], and has already eliminated a wide range of the parameter space.

As a related subject, H. Miyake (Tsukuba) is involved in the $B_s^0$ meson lifetime and width difference measurement using the semileptonic decays $\bar{B}_s^0 \to \ell^- \bar{\nu} D_s^+ X$.

Also, J. Naganoma and H. Miyake (Tsukuba) are searching for the rare, FCNC decays $B_s^0 \to \mu^+\mu^-$ and $B \to K^{(*)}\ell^+\ell^-$.

## 1.4 New particle searches

Searches for the Higgs boson, supersymmetric particles and other new particles have been performed. Cross sections for the standard model Higgs boson production at the Tevatron is shown in Figure 9 (left) for various subprocesses. The largest contribution comes from the single production through gluon fusion, with the top quark in the loop. Associated production with a weak boson, $W^{\pm}H$ and $Z^0H$, is smaller. The decay branching fractions of the Higgs boson are shown in Figure 9 (right). At a low mass, below 135 GeV/$c^2$, the decay to $b\bar{b}$ pairs is dominant, while at a high mass the decays to weak boson pairs become dominant.

CDF has searched for the Higgs boson production using many different final states. The first, aimed at a low mass Higgs, looks for the associated production $\bar{p}p \to VHX$, where $V$ is a weak gauge boson $W^{\pm}$ or $Z^0$, with the $W^{\pm}$ ($Z^0$) boson decaying into $\ell^{\pm}\nu$ ($\ell^+\ell^-$, $\nu\bar{\nu}$) pairs, and the Higgs boson to $b\bar{b}$ pairs. The $b$ quark jets are identified with displaced vertices. The main background comes from heavy flavor ($b\bar{b}$, $c\bar{c}$) production in association with the vector boson $V$, and top quark pair production. Various kinematic distributions, including the di-jet mass distribution (Figure 11 (left)), are examined for possible production of the Higgs boson. Also an artificial neural network discriminant is employed (Figure 11 (right)). No excess of events over known backgrounds is found in 2.7 fb$^{-1}$ of data, and upper limits on the Higgs boson production cross section are set, in the range of 3.7 to 60 times the standard model value, depending on the assumed Higgs boson mass (110 to 150 GeV/$c^2$) [9]. Y. Nagai (Tsukuba) has performed the analysis and extended the search using the electrons produced in the endplug region. M. Kurata (Tsukuba) is applying the Dynamical Likelihood Method to the Higgs search in this channel.

The second analysis looks for single production of the Higgs boson followed by its decays to $W$ boson pairs. The channel is sensitive to a high mass Higgs. The $W^+W^-$ final state is identified with their decays to leptons, thus the signature is two energetic leptons and a large missing transverse energy and nothing else. The dominant background comes from electroweak $W^+W^-$ production, which leads to the same signature. However, there exists a difference in event topology, for example the lepton azimuthal angle correlations. Again, no excess of events is observed and upper limits on Higgs production have been placed. This is presently the most sensitive search channel at CDF, and the upper limits for masses around 160 GeV/$c^2$ are less than twice the Standard Model values.

The third method looks for associated production of the Higgs boson with a weak boson $W^{\pm}$ or $Z^0$, where the Higgs boson decays to $W^+W^-$ boson pair and one or both of the $W$ boson can be off mass shell. There exist three weak bosons in the final state, where two of them have the same charge. They are required to decay leptonically, leading to a very distinctive final state of isolated, same-charge lepton pairs, such as $e^+\mu^+$. A boosted-decision tree technique has been employed to improve sensitivity, of which example outputs are shown in Figure ??. No significant excess of events are observed over the expected backgrounds, and upper limits on production cross sections are placed [10]. T. Wakisaka (Osaka City) has performed the analysis for his Ph.D. thesis.

The results from different analyses are combined and summarized in Figure 12, where the obtained upper limits on cross sections are normalized to standard model predictions. The limits are within a factor of two for a Higgs mass near 160 GeV/$c^2$, and are about a factor of three to four at low mass [11]. Figure 13 shows the limits where the results from both CDF and D0 experiments are combined. Data up to 4.2 fb$^{-1}$ have been analyzed. A mass range between 160 GeV/$c^2$ and 170 GeV/$c^2$ has been excluded at 95% CL [12] for the first time.

# References


[1] "First Measurement of the $W$-boson mass in Run II of the Tevatron",
CDF Collaboration, T. Aaltonen *et al.*, Phys. Rev. Lett. **99**, 151801 (2007).
"First Run II measurement of the $W$ boson mass at the Fermilab Tevatron",
CDF Collaboration, T. Aaltonen *et al.*, Phys. Rev. D **77**, 112001 (2008).

[2] "Combination of CDF top quark pair production cross section measurements with 2.8 fb$^{-1}$",
CDF Collaboration, CDF public note 9448 (2008).

[3] "Combination of CDF top quark mass measurements using up to 3.2 fb$^{-1}$",
CDF Collaboration, CDF public note 9714 (2009).

[4] "Measurement of the gluon fusion fraction in $t\bar{t}$ production using azimuthal correlation of charged leptons",
CDF Collaboration, CDF public note 9432 (2008).
"Study of the Top Quark Production Mechanism in 1.96-TeV Proton-Antiproton Collisions",
Naoki Kimura, Ph. D. Thesis, University of Tsukuba, February 2009.

[5] "Search for single top quark production optimized for $s$-channel production with 3.2 fb$^{-1}$ data",
CDF Collaboration, CDF public note 9712 (2009).
"Measurement of the Single Top Quark Production Cross Section in 1.96-TeV Proton-Antiproton Collisions",
Koji Nakamura, Ph. D. Thesis, University of Tsukuba, February 2009.

[6] "Measurement of the single top quark production cross section at CDF",
T. Aaltonen *et al.*, Phys. Rev. Lett. **101**, 252001 (2008).
"First observation of electroweak single top quark production",
T. Aaltonen *et al.*, arXiv:0903.0885 [hep-ex] (2009).

[7] "Observation of $B_s^0$-$\bar{B}_s^0$ Oscillations",
A. Abulencia *et al.*, Phys. Rev. Lett. **97**, 242003 (2006).
"Measurement of the $B_s^0$-$\bar{B}_s^0$ Oscillation Frequency",
A. Abulencia *et al.*, Phys. Rev. Lett. **97**, 062003 (2006).

[8] "Measurement of Lifetime and Decay-Width Difference in $B_s^0 \to J/\psi\,\phi$ Decays",
T. Aaltonen *et al.*, Phys. Rev. Lett. **100**, 121803 (2008).
"First Flavor-Tagged Determination of Bounds on Mixing-Induced CP Violation in $B_s^0 \to J/\psi\,\phi$ Decays",
T. Aaltonen *et al.*, Phys. Rev. Lett. **100**, 161802 (2008).
"An updated measurement of the CP violating phase $\beta_s^{J/\psi\phi}$",
CDF Collaboration, CDF public note 9458 (2008).

[9] "Search for standard model Higgs boson production in association with $W^{\pm}$ boson at CDF with 2.7 fb$^{-1}$",
CDF Collaboration, CDF public note 9468 (2008).

[10] "Search for the $WH$ Production Using High-$p_{\mathrm{T}}$ Isolated Like-sign Dilepton Events in Run II",
Takayuki Wakisaka, Ph. D. Thesis, Osaka City University, February 2009.

[11] "Combined upper limit on standard model Higgs boson production at CDF for winder 2009",
CDF Collaboration, CDF public web page at
http://www-cdf.fnal.gov/physics/new/hdg/combcdf_090116/ (2009).

[12] "Combined CDF and D0 upper limits on standard model Higgs-boson production with up to 4.2 fb$^{-1}$ of data",
CDF and D0 Collaborations, CDF public note 9713 (2009).

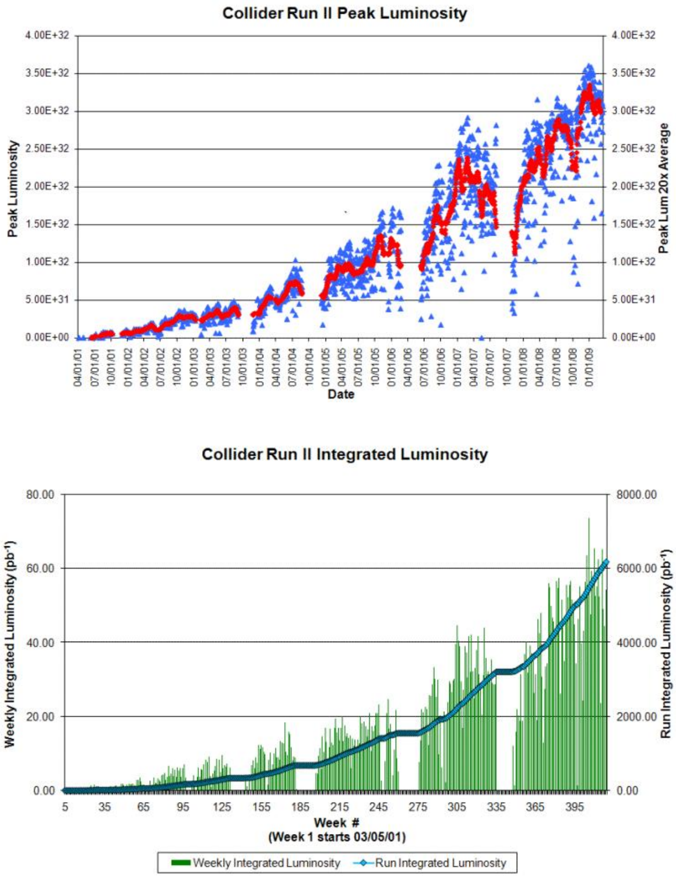


Figure 1: Tevatron performance in Run II. Top: instantaneous luminosity at the beginning of each store. Bottom: integrated luminosity delivered by week.

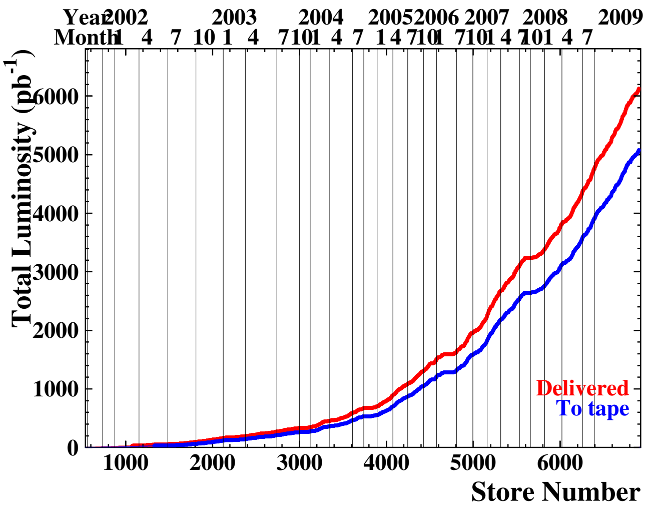


Figure 2: Integrated luminosity (top) delivered to and (bottom) recorded by CDF in Tevatron Run II.

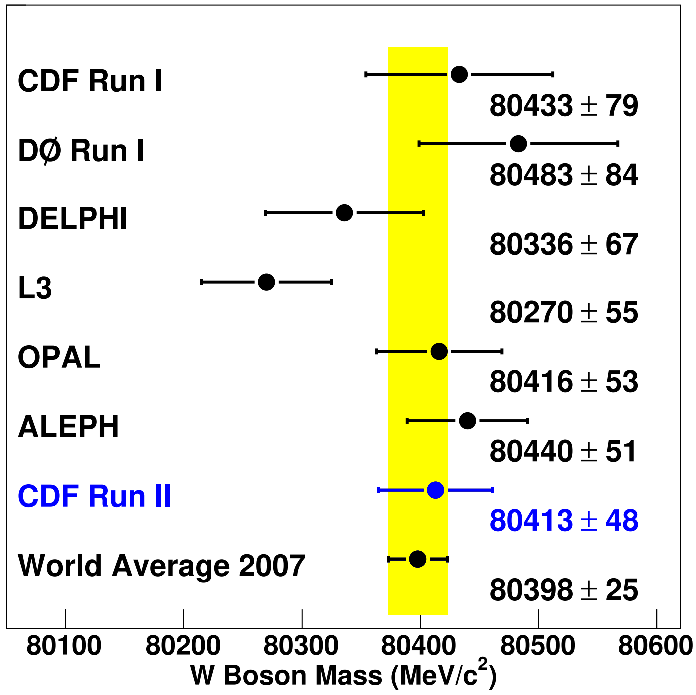


Figure 3: A summary of $W^{\pm}$ boson mass measurements.

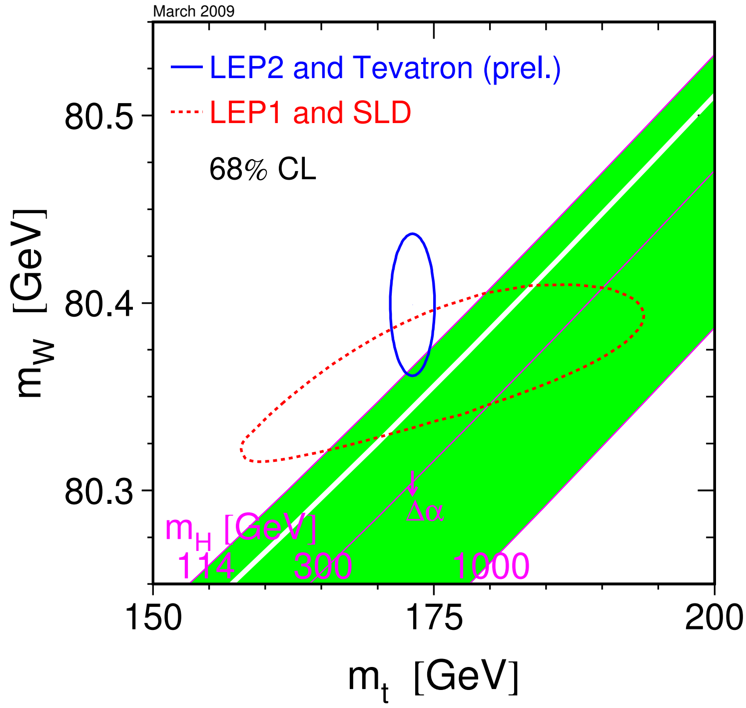


Figure 4: Measurements of the top quark and $W$ boson masses as of March 2009, and indirect information on the Higgs boson mass.

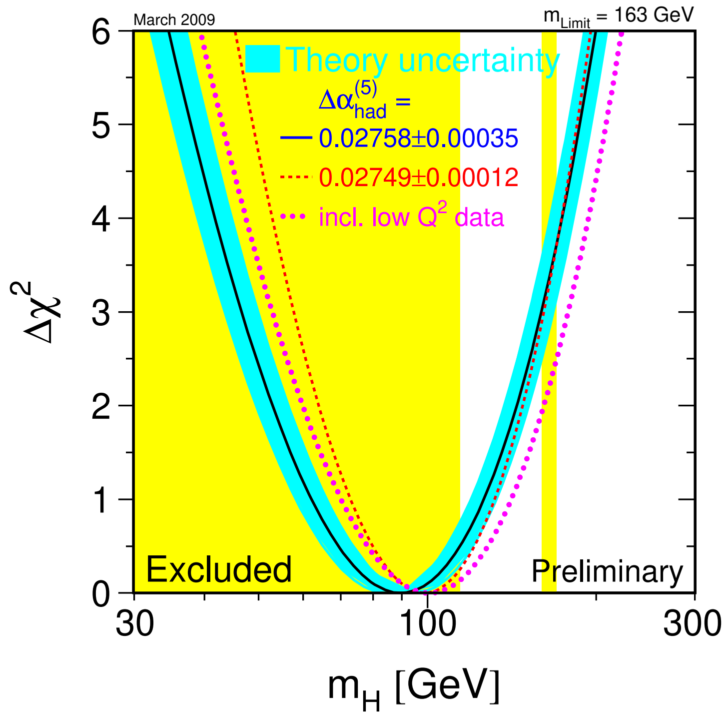


Figure 5: Likelihood distribution for the Higgs boson mass derived from global fits to electroweak measurements.

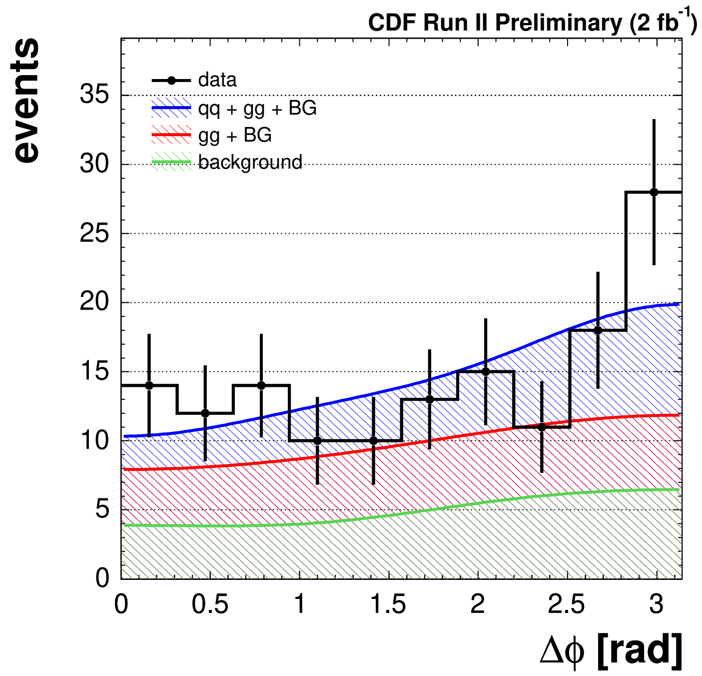


Figure 6: Study of $t\bar{t}$ production mechanism. Two parton subprocesses, $q\bar{q} \to t\bar{t}$ and $gg \to t\bar{t}$, are distinguished using the correlations in $t\bar{t}$ spin states and resultant azimuthal angles of two charged leptons.

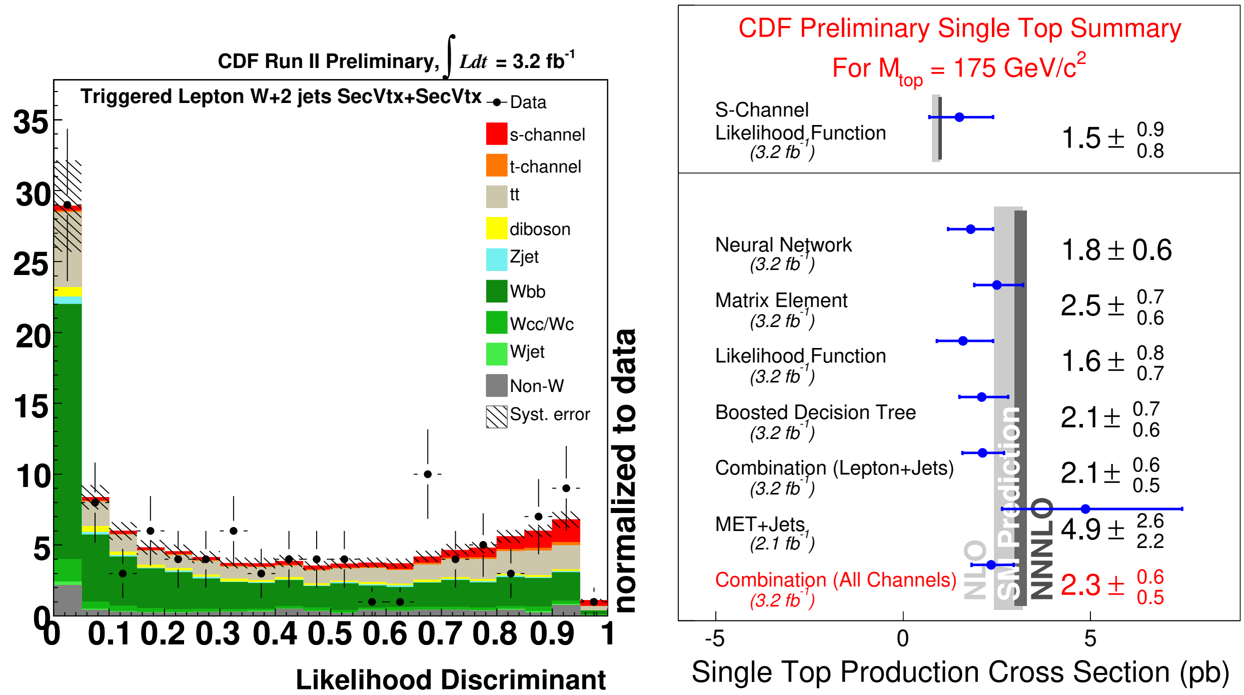


Figure 7: Search for single top-quark production. Left: Likelihood discriminant distribution for $s$-channel search. Right: Summary of single top-quark production cross section from various analyses.

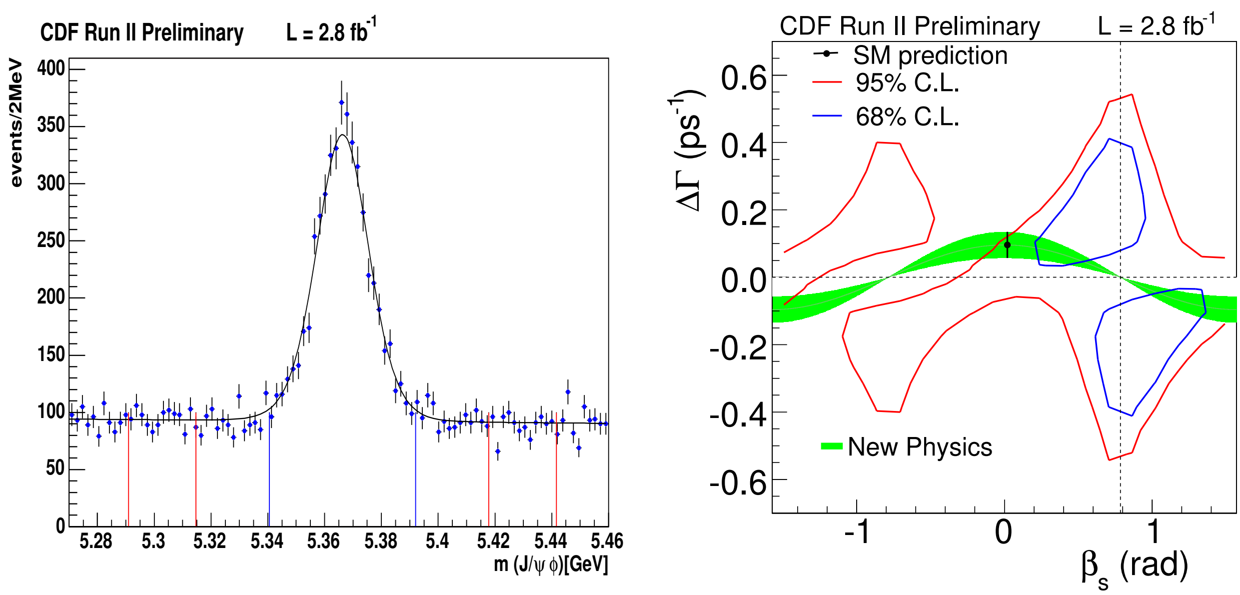


Figure 8: Search for CP violation in $B_s^0$-$\bar{B}_s^0$ mixing. Left: $B_s^0$ meson signal in $B_s^0 \to J/\psi\,\phi$ mode. Right: Constraints obtained on the CP-violating phase $\beta_s$ and the width difference $\Delta\Gamma_s$, as well as the standard model prediction.

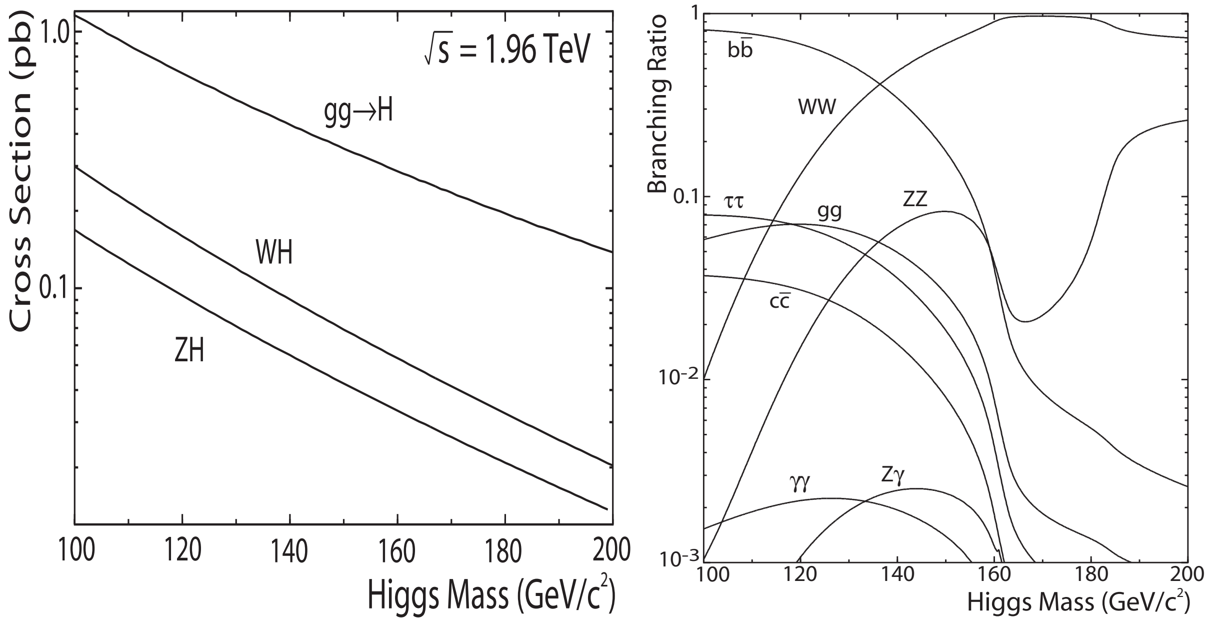


Figure 9: Left: Cross section for the production of the standard model Higgs boson at Tevatron. right: Branching fractions of the standard model Higgs boson to various final states. Both plots show dependences on the Higgs boson mass.

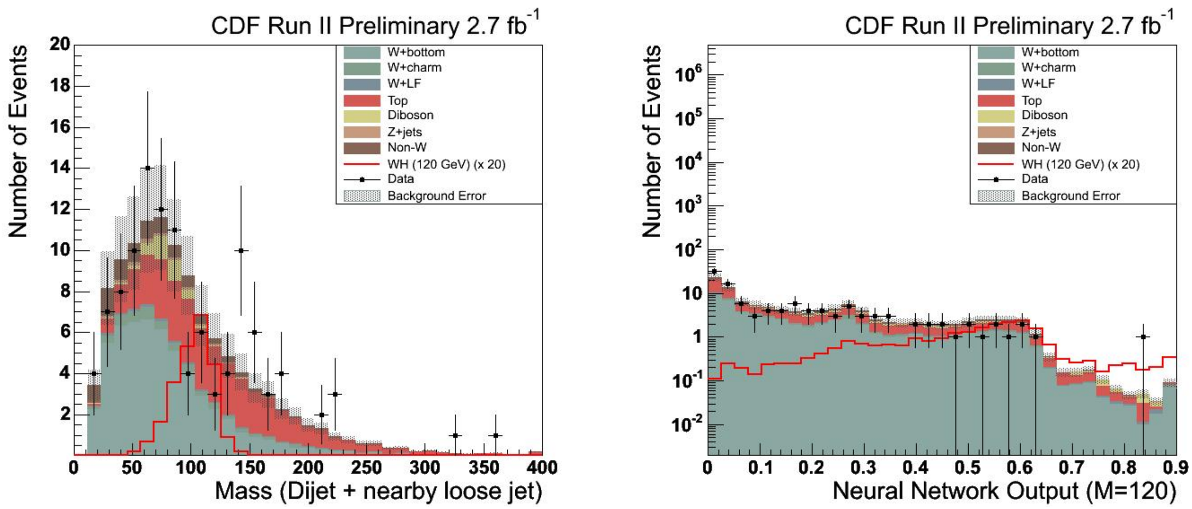


Figure 10: Higgs boson search in the $p\bar{p} \to W^{\pm}HX \to (\ell^{\pm}\nu)\,(b\bar{b})\,X$ channel. Left: Invariant mass distribution of the two $b$-quark candidate jets produced in association with a $W$ boson. Right: Output of the artificial neural network discriminant.

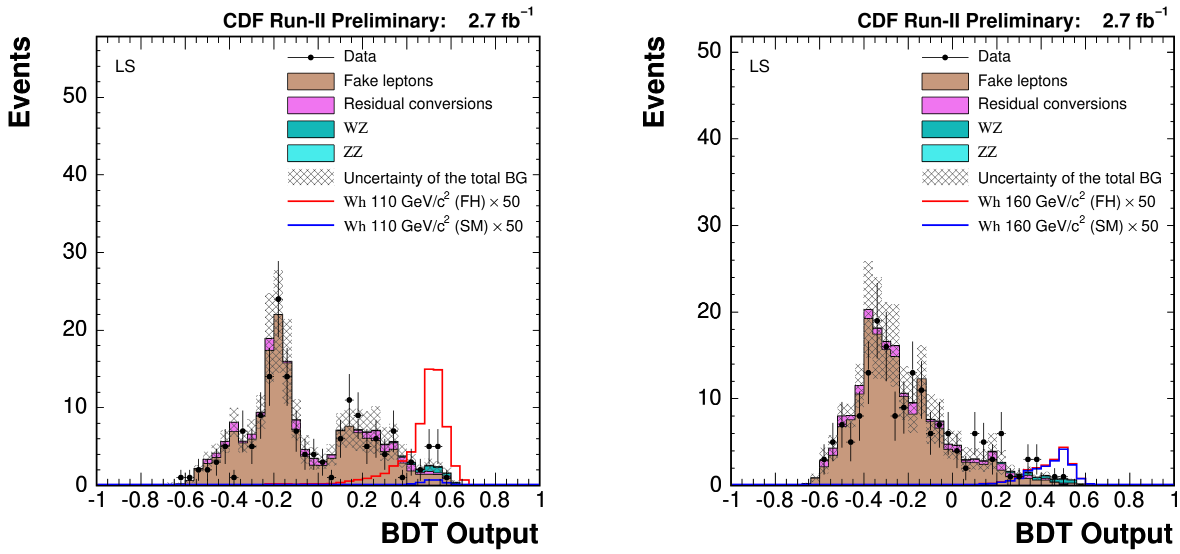


Figure 11: Output distribution of the Boosted Decision Tree analysis in the Higgs boson search using the $p\bar{p} \to W^{\pm}HX \to WWWX \to \ell^{\pm}\ell'^{\pm}X'$ channel, for an assumed Higgs mass of 110 GeV/$c^2$ and 160 GeV/$c^2$.

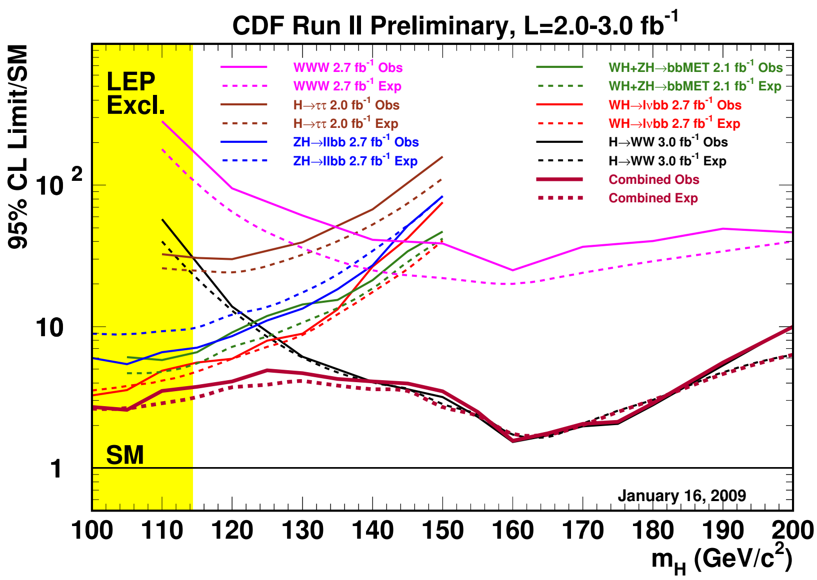


Figure 12: Summary of CDF results on the searches for the standard model Higgs boson. The experimental upper limits on production cross sections, normalized to the theoretical predictions, are shown for all search channels.

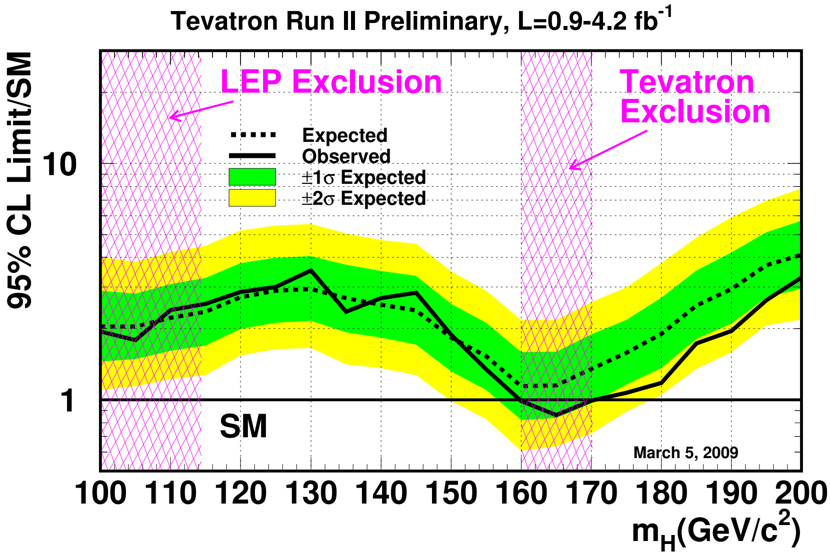


Figure 13: Summary of combined CDF and D0 results on the searches for the standard model Higgs boson. The experimental upper limits on production cross sections, normalized to the theoretical predictions, are shown after combining all search channels. The mass range between 160 GeV/$c^2$ and 170 GeV/$c^2$ has been excluded at 95% CL.